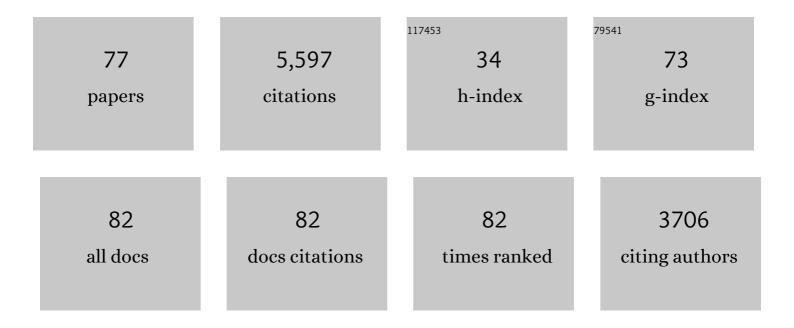
## Nicholas Cox

List of Publications by Year in descending order

Source: https://exaly.com/author-pdf/6135590/publications.pdf Version: 2024-02-01



#	Article	IF	CITATIONS
1	The syntheses, structures and spectroelectrochemical properties of 6-oxo-verdazyl derivatives bearing surface anchoring groups. Journal of Materials Chemistry C, 2022, 10, 1896-1915.	2.7	7
2	Crystalline Germanium(I) and Tin(I) Centered Radical Anions. Angewandte Chemie, 2022, 134, .	1.6	4
3	Crystalline Germanium(I) and Tin(I) Centered Radical Anions. Angewandte Chemie - International Edition, 2022, 61, .	7.2	13
4	Redoxâ€Addressable Singleâ€Molecule Junctions Incorporating a Persistent Organic Radical**. Angewandte Chemie - International Edition, 2022, 61, .	7.2	25
5	Defect engineering for creating and enhancing bulk photovoltaic effect in centrosymmetric materials. Journal of Materials Chemistry A, 2021, 9, 13182-13191.	5.2	12
6	A Chiral Lanthanide Tag for Stable and Rigid Attachment to Single Cysteine Residues in Proteins for NMR, EPR and Timeâ€Resolved Luminescence Studies. Chemistry - A European Journal, 2021, 27, 13009-13023.	1.7	19
7	Enhanced Synthesis of oxo-Verdazyl Radicals Bearing Sterically-and Electronically-Diverse C3-Substitents. Organic and Biomolecular Chemistry, 2021, 19, 10120-10138.	1.5	6
8	Microwave Dielectric Materials with Defect-Dipole Clusters Induced Colossal Permittivity and Ultra-low Loss. ACS Applied Electronic Materials, 2021, 3, 5015-5022.	2.0	8
9	Hole-Pinned Defect Clusters for a Large Dielectric Constant up to GHz in Zinc and Niobium Codoped Rutile SnO <sub>2</sub> . ACS Applied Materials & Interfaces, 2021, 13, 54124-54132.	4.0	9
10	Substituent Effects on Photoinitiation Ability of Monoaminoanthraquinoneâ€Based Photoinitiating Systems for Free Radical Photopolymerization under LEDs. Macromolecular Rapid Communications, 2020, 41, e2000166.	2.0	11
11	Free Radical Generation from High-Frequency Electromechanical Dissociation of Pure Water. Journal of Physical Chemistry Letters, 2020, 11, 4655-4661.	2.1	23
12	The primary donor of far-red photosystem II: ChlD1 or PD2?. Biochimica Et Biophysica Acta - Bioenergetics, 2020, 1861, 148248.	0.5	19
13	Current Understanding of the Mechanism of Water Oxidation in Photosystem II and Its Relation to XFEL Data. Annual Review of Biochemistry, 2020, 89, 795-820.	5.0	123
14	New Perspectives on Photosystem II Reaction Centres. Australian Journal of Chemistry, 2020, 73, 669.	0.5	6
15	Defect structure and property consequence when small Li+ ions meet BaTiO3. Physical Review Materials, 2020, 4, .	0.9	1
16	Five-coordinate Mn <sup>IV</sup> intermediate in the activation of nature's water splitting cofactor. Proceedings of the National Academy of Sciences of the United States of America, 2019, 116, 16841-16846.	3.3	54
17	In Situ EPR Characterization of a Cobalt Oxide Water Oxidation Catalyst at Neutral pH. Catalysts, 2019, 9, 926.	1.6	27
18	Water oxidation in photosystem II. Photosynthesis Research, 2019, 142, 105-125.	1.6	149

#	Article	IF	CITATIONS
19	Chemical flexibility of heterobimetallic Mn/Fe cofactors: R2lox and R2c proteins. Journal of Biological Chemistry, 2019, 294, 18372-18386.	1.6	8
20	Structural adaptations of photosynthetic complex I enable ferredoxin-dependent electron transfer. Science, 2019, 363, 257-260.	6.0	162
21	Highly Efficient Visible Light Catalysts Driven by Ti <sup>3+</sup> â€V <sub>O</sub> â€2Ti <sup>4+</sup> â€N <sup>3â^'</sup> Defect Clusters. ChemNanoMat, 2 5, 169-174.	20 <b>1.9</b> ,	3
22	Oxygen-deficient photostable Cu <sub>2</sub> O for enhanced visible light photocatalytic activity. Nanoscale, 2018, 10, 6039-6050.	2.8	115
23	Structured near-infrared Magnetic Circular Dichroism spectra of the Mn4CaO5 cluster of PSII in T. vulcanus are dominated by Mn(IV) d-d †spin-flip' transitions. Biochimica Et Biophysica Acta - Bioenergetics, 2018, 1859, 88-98.	0.5	12
24	Biomolecular EPR Meets NMR at High Magnetic Fields. Magnetochemistry, 2018, 4, 50.	1.0	21
25	Disubstituted Aminoanthraquinone-Based Photoinitiators for Free Radical Polymerization and Fast 3D Printing under Visible Light. Macromolecules, 2018, 51, 10104-10112.	2.2	38
26	Metal-free ribonucleotide reduction powered by a DOPA radical in Mycoplasma pathogens. Nature, 2018, 563, 416-420.	13.7	50
27	What Can We Learn from a Biomimetic Model of Nature's Oxygen-Evolving Complex?. Inorganic Chemistry, 2017, 56, 3875-3888.	1.9	40
28	Solvent water interactions within the active site of the membrane type I matrix metalloproteinase. Physical Chemistry Chemical Physics, 2017, 19, 30316-30331.	1.3	16
29	The First State in the Catalytic Cycle of the Water-Oxidizing Enzyme: Identification of a Water-Derived μ-Hydroxo Bridge. Journal of the American Chemical Society, 2017, 139, 14412-14424.	6.6	63
30	ELDOR-detected NMR: A general and robust method for electron-nuclear hyperfine spectroscopy?. Journal of Magnetic Resonance, 2017, 280, 63-78.	1.2	35
31	Divergent assembly mechanisms of the manganese/iron cofactors in R2lox and R2c proteins. Journal of Inorganic Biochemistry, 2016, 162, 164-177.	1.5	24
32	Recent developments in biological water oxidation. Current Opinion in Chemical Biology, 2016, 31, 113-119.	2.8	97
33	A five-coordinate Mn( <scp>iv</scp> ) intermediate in biological water oxidation: spectroscopic signature and a pivot mechanism for water binding. Chemical Science, 2016, 7, 72-84.	3.7	158
34	Spin State as a Marker for the Structural Evolution of Nature's Water-Splitting Catalyst. Inorganic Chemistry, 2016, 55, 488-501.	1.9	87
35	Pulse Double-Resonance EPR Techniques for the Study of Metallobiomolecules. Methods in Enzymology, 2015, 563, 211-249.	0.4	16
36	Artificial photosynthesis: understanding water splitting in nature. Interface Focus, 2015, 5, 20150009.	1.5	60

#	Article	IF	CITATIONS
37	Metal oxidation states in biological water splitting. Chemical Science, 2015, 6, 1676-1695.	3.7	275
38	Redox-dependent Ligand Switching in a Sensory Heme-binding GAF Domain of the Cyanobacterium Nostoc sp. PCC7120. Journal of Biological Chemistry, 2015, 290, 19067-19080.	1.6	14
39	Characterization of Oxygen Bridged Manganese Model Complexes Using Multifrequency <sup>17</sup> O-Hyperfine EPR Spectroscopies and Density Functional Theory. Journal of Physical Chemistry B, 2015, 119, 13904-13921.	1.2	27
40	Nitrite Dismutase Reaction Mechanism: Kinetic and Spectroscopic Investigation of the Interaction between Nitrophorin and Nitrite. Journal of the American Chemical Society, 2015, 137, 4141-4150.	6.6	22
41	Structure, ligands and substrate coordination of the oxygen-evolving complex of photosystem II in the S2 state: a combined EPR and DFT study. Physical Chemistry Chemical Physics, 2014, 16, 11877.	1.3	77
42	The first tyrosyl radical intermediate formed in the S2–S3 transition of photosystem II. Physical Chemistry Chemical Physics, 2014, 16, 11901.	1.3	68
43	A First-Principles Approach to the Calculation of the on-Site Zero-Field Splitting in Polynuclear Transition Metal Complexes. Inorganic Chemistry, 2014, 53, 11785-11793.	1.9	32
44	The D1-173 amino acid is a structural determinant of the critical interaction between D1-Tyr161 (TyrZ) and D1-His190 in Photosystem II. Biochimica Et Biophysica Acta - Bioenergetics, 2014, 1837, 1922-1931.	0.5	16
45	Electronic Structural Flexibility of Heterobimetallic Mn/Fe Cofactors: R2lox and R2c Proteins. Journal of the American Chemical Society, 2014, 136, 13399-13409.	6.6	37
46	Electronic structure of the oxygen-evolving complex in photosystem II prior to O-O bond formation. Science, 2014, 345, 804-808.	6.0	432
47	EPR Spectroscopy and the Electronic Structure of the Oxygen-Evolving Complex of Photosystem II. Applied Magnetic Resonance, 2013, 44, 691-720.	0.6	24
48	Ammonia binding to the oxygen-evolving complex of photosystem II identifies the solvent-exchangeable oxygen bridge (μ-oxo) of the manganese tetramer. Proceedings of the National Academy of Sciences of the United States of America, 2013, 110, 15561-15566.	3.3	148
49	Direct observation of structurally encoded metal discrimination and ether bond formation in a heterodinuclear metalloprotein. Proceedings of the National Academy of Sciences of the United States of America, 2013, 110, 17189-17194.	3.3	49
50	W-band ELDOR-detected NMR (EDNMR) spectroscopy as a versatile technique for the characterisation of transition metal–ligand interactions. Molecular Physics, 2013, 111, 2788-2808.	0.8	59
51	Reflections on substrate water and dioxygen formation. Biochimica Et Biophysica Acta - Bioenergetics, 2013, 1827, 1020-1030.	0.5	234
52	Biological Water Oxidation. Accounts of Chemical Research, 2013, 46, 1588-1596.	7.6	453
53	Molecular Concepts of Water Splitting: Nature's Approach. Green, 2013, 3, .	0.4	2
54	Detection of the Water-Binding Sites of the Oxygen-Evolving Complex of Photosystem II Using W-Band <sup>17</sup> O Electron–Electron Double Resonance-Detected NMR Spectroscopy. Journal of the American Chemical Society, 2012, 134, 16619-16634.	6.6	248

#	Article	IF	CITATIONS
55	Two Interconvertible Structures that Explain the Spectroscopic Properties of the Oxygenâ€Evolving Complex of Photosystemâ€II in the S <sub>2</sub> State. Angewandte Chemie - International Edition, 2012, 51, 9935-9940.	7.2	342
56	What Are the Oxidation States of Manganese Required To Catalyze Photosynthetic Water Oxidation?. Biophysical Journal, 2012, 103, 313-322.	0.2	72
57	The Basic Properties of the Electronic Structure of the Oxygen-evolving Complex of Photosystem II Are Not Perturbed by Ca2+ Removal. Journal of Biological Chemistry, 2012, 287, 24721-24733.	1.6	56
58	Charge separation in Photosystem II: A comparative and evolutionary overview. Biochimica Et Biophysica Acta - Bioenergetics, 2012, 1817, 26-43.	0.5	293
59	Electronic Structure of a Weakly Antiferromagnetically Coupled Mn <sup>II</sup> Mn <sup>III</sup> Model Relevant to Manganese Proteins: A Combined EPR, <sup>55</sup> Mn-ENDOR, and DFT Study. Inorganic Chemistry, 2011, 50, 8238-8251.	1.9	55
60	Semiquinone–Iron Complex of Photosystem II: EPR Signals Assigned to the Low-Field Edge of the Ground State Doublet of Q <sub>A</sub> <sup>•–</sup> Fe <sup>2+</sup> and Q <sub>B</sub> <sup>•–</sup> Fe <sup>2+</sup> . Biochemistry, 2011, 50, 6012-6021.	1.2	27
61	Effect of Ca <sup>2+</sup> /Sr <sup>2+</sup> Substitution on the Electronic Structure of the Oxygen-Evolving Complex of Photosystem II: A Combined Multifrequency EPR, <sup>55</sup> Mn-ENDOR, and DFT Study of the S <sub>2</sub> State. Journal of the American Chemical Society, 2011, 133, 3635-3648.	6.6	211
62	Theoretical Evaluation of Structural Models of the S <sub>2</sub> State in the Oxygen Evolving Complex of Photosystem II: Protonation States and Magnetic Interactions. Journal of the American Chemical Society, 2011, 133, 19743-19757.	6.6	271
63	Effects of formate binding on the quinone–iron electron acceptor complex of photosystem II. Biochimica Et Biophysica Acta - Bioenergetics, 2011, 1807, 216-226.	0.5	30
64	The electronic structures of the S2 states of the oxygen-evolving complexes of photosystem II in plants and cyanobacteria in the presence and absence of methanol. Biochimica Et Biophysica Acta - Bioenergetics, 2011, 1807, 829-840.	0.5	81
65	D1 protein variants in Photosystem II from Thermosynechococcus elongatus studied by low temperature optical spectroscopy. Biochimica Et Biophysica Acta - Bioenergetics, 2010, 1797, 11-19.	0.5	21
66	On the assignment of PSHB in D1/D2/ cytb559 reaction centers. Physics Procedia, 2010, 3, 1601-1605.	1.2	9
67	Homologous expression of the <i>nrdF</i> gene of <i>Corynebacteriumâ€fammoniagenes</i> strainâ€fATCCâ€f6872 generates a manganeseâ€metallocofactor (R2F) and a stable tyrosyl radical (Y <sup>•</sup> ) involved in ribonucleotide reduction. FEBS Journal, 2010, 277, 4849-4862.	2.2	21
68	A Tyrosylâ^'Dimanganese Coupled Spin System is the Native Metalloradical Cofactor of the R2F Subunit of the Ribonucleotide Reductase of Corynebacterium ammoniagenes. Journal of the American Chemical Society, 2010, 132, 11197-11213.	6.6	93
69	Intramolecular light induced activation of a Salen–MnIII complex by a ruthenium photosensitizer. Chemical Communications, 2010, 46, 7605.	2.2	29
70	The S1 split signal of photosystem II; a tyrosine–manganese coupled interaction. Biochimica Et Biophysica Acta - Bioenergetics, 2009, 1787, 882-889.	0.5	12
71	Photo-catalytic oxidation of a di-nuclear manganese centre in an engineered bacterioferritin â€~reaction centre'. Biochimica Et Biophysica Acta - Bioenergetics, 2009, 1787, 1112-1121.	0.5	42
72	Identification of the Q <sub><i>Y</i></sub> Excitation of the Primary Electron Acceptor of Photosystem II: CD Determination of Its Coupling Environment. Journal of Physical Chemistry B, 2009, 113, 12364-12374.	1.2	27

73The Semiquinone-Iron Complex of Photosystem II: Structural Insights from ESR and Theoretical Simulation; Evidence that the Native Ligand to the Non-Heme Iron Is Carbonate. Biophysical Journal, 2009, 97, 2024-2033.0.23474Spectral characteristics of PS II reaction centres: as isolated preparations and when integral to PS II core complexes. Photosynthesis Research, 2008, 98, 207-217.1.62775The FT-IR spectra of glycine and glycylglycine zwitterions isolated in alkali halide matrices. Chemical0.070	#	IF CITATIONS
The ET-IR spectra of glycine and glycy/glycine zwitterions isolated in alkali halide matrices. Chemical	73	tructural Insights from ESR and Theoretical Non-Heme Iron Is Carbonate. Biophysical Journal, 0.2 34
The FT-IR spectra of glycine and glycylglycine zwitterions isolated in alkali halide matrices. Chemical	74	isolated preparations and when integral to PS II 1.6 27 3, 207-217.
<sup>75</sup> Physics, 2005, 313, 39-49.	75	erions isolated in alkali halide matrices. Chemical 0.9 70
76 Dielectric Coupler for General Purpose Q-Band EPR Cavity. Applied Magnetic Resonance, 0, , 1. 0.6 1	76	Cavity. Applied Magnetic Resonance, 0, , 1. 0.6 1
<ul> <li>Redoxâ€Addressable Singleâ€Molecule Junctions Incorporating a Persistent Organic Radical**.</li> <li>1.6 0</li> </ul>	77	corporating a Persistent Organic Radical**. 1.6 O